ACS APPLIED MATERIALS & INTERFACES

Research Article

www.acsami.org

Formation of Layer-by-Layer Assembled Titanate Nanotubes Filled Coating on Flexible Polyurethane Foam with Improved Flame Retardant and Smoke Suppression Properties

Haifeng Pan,[†,‡] Wei Wang,[†] Ying Pan,[†] Lei Song,[*,†] Yuan Hu,[*,†,‡] and Kim Meow Liew[‡,§]

[†]State Key Laboratory of Fire Science, University of Science and Technology of China, 96 Jinzhai Road, Hefei, Anhui 230026, People's Republic of China

[‡]Suzhou Key Laboratory of Urban Public Safety, Suzhou Institute of University of Science and Technology of China, 166 Ren'ai Road, Suzhou, Jiangsu 215123, People's Republic of China

[§]Department of Building and Construction, City University of Hong Kong, Tat Chee Avenue Kowloon, Hong Kong, People's Republic of China

Supporting Information

ABSTRACT: A fire blocking coating made from chitosan, titanate nanotubes and alginate was deposited on a flexible polyurethane (FPU) foam surface by a layer-by-layer assembly technique in an effort to reduce its flammability. First, titanate nanotubes were prepared by a hydrothermal method. And then the coating growth was carried out by alternately submerging FPU foams into chitosan solution, titanate nanotubes suspension and alginate solution. The mass gain of coating on the surface of FPU foams showed dependency on the concentration of titanate nanotubes suspension and the trilayers's number. Scanning electron microscopy indicated that titanate nanotubes were distributed well on the entire surface of FPU foam and showed a randomly oriented and entangled network structure. The cone calorimeter result indicated that the coated FPU foams showed reduction in the peak heat release rate (peak HRR), peak smoke production rate (peak SPR), total smoke release (TSR) and peak carbon monoxide (CO) production compared with those of the control FPU foam. Especially for the FPU foam with only 5.65 wt % mass gain, great reduction in peak HRR (70.2%), peak SPR (62.8%), TSR (40.9%) and peak CO production (63.5%) could be observed. Such a significant improvement in flame retardancy and the smoke suppression property for FPU foam could be attributed to the protective effect of titanate nanotubes network structure formed, including insulating barrier effect and adsorption effect.

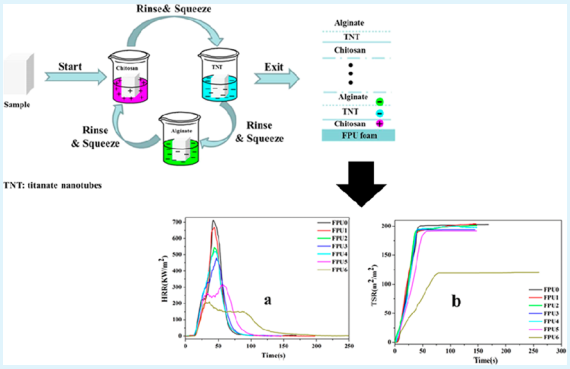

KEYWORDS: *layer-by-layer assembled method, titanate nanotubes, flame retardancy, smoke suppression, insulating barrier effect, adsorption effect*

INTRODUCTION

Titanium oxide (TiO_2) and its derivative materials are widely being studied in various applications, such as batteries, separations and photocatalysis. Recently, one-dimensional titanium oxide materials, titanate nanotubes, have attracted much attention due to the nonlinear optical properties, intriguing physicochemical and high surface area.[1,2] These properties render titanate nanotubes suitable for various applications, including catalysis, electrocatalysis and photocatalysis.[3−5] The extensive research on the potential application of titanate nanotubes as a flame retardant additive has been carried out due to the excellent protective effect of network structure formed.[6,7] Generally speaking, controlling the dispersion of nanotubes materials in polymeric materials is important for effectively adjusting the network structure and subsequent protective effect. On the basis of this, our research group introduced phenyl dichlorophosphate (PDCP) surface modified TiO_2 nanotubes into an epoxy resin, in which the PDCP modified TiO_2 nanotubes dispersed homogeneously and the nanotubes formed network structure acted as an effective barrier to resist the release of flammable gases and change degradation pathway.[6] Additionally, in situ polymerization of methyl methacrylate monomers along with titanate nanotubes was also carried out by our group, and the nanocomposites showed an excellent smoke suppression property owing to the excellent adsorption effect of titanate nanotubes (titanate nanotubes are usually found to be open-ended scrolls with a tubular structure and have a large specific surface area).[7] In fact, the oxygen adsorption capacity of titanate nanotubes as the component of an oxygen sensor has been widely used.[8,9] The

Received: May 24, 2014
Accepted: December 12, 2014
Published: December 12, 2014

Scheme 1. Schematic of the Layer-by-Layer Assembled Process for Construction of Chitosan/Titanate Nanotubes/Alginate Coating on FPU Foams

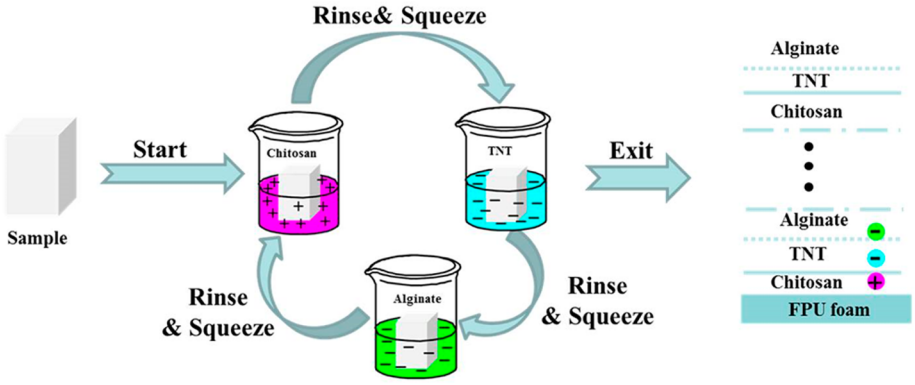

TNT: titanate nanotubes

layer-by-layer (LbL) assembly technique can be used to incorporate various polymers, colloids or molecules into a thin film most often through electrostatic attraction. It can fabricate a thin film on the substrate with good dispersion and controlled properties. Titanate nanotubes with a hydrogen titanate structure can show the negatively charged nanoparticles in aqueous solution owing to its protonic nature.[10,11] In fact, the titanate nanotubes filled multilayer films have been fabricated by Langmuir−Blodgett and layer-by-layer assembled techniques.[12−14] Here, such a multilayer film was used to be deposited on FPU foam surface to improve the fire safety by layer-by-layer (LbL) assembly.

Previous works have reported some typical flame retardant multilayer films on FPU foam.[15−19] FPU foams are widely used as the comfort component in consumer furniture, mattresses and buildings. They are highly flammable materials, which can be the cause of a small fire rapidly developing into a significant fire threat. Therefore, it is of significance to improve its flame retardant properties. First, the carbon nanofibers filled LbL flame retardant coating was deposited on FPU foam by Kim et al.[15] Subsequently, some typical inorganic nanoparticles, including montmorillonite (MMT) and carbon nanotubes (CNTs), were studied to as the effective flame retardant coating on FPU foam.[16−18] However, the flame retardant efficiency is not very notable: high loading level of coating mass must be provided to significantly reduce the flammability of FPU foam. Additionally, their works were scarcely focused on the investigation of smoke property, which is important property for FPU foam due to the fact that polyether units of foam thermally degrade and regenerate isocyanate and diol precursor groups, producing large amount of harmful smoke and combustion products.

It should be noted that Kim et al. failed to fabricate an MMT filled flame retardant coating on FPU foam according to the traditional bilayers's approach (polyethylenimine (PEI)/MMT). The coating had only about 1% mass gain and 100 nm thickness when 20 bilayers were fabricated on FPU foam. At the same time, a novel approach, named the trilayers approach, was used to carry out the relative works (polyethylenimine (PEI)/MMT/poly(acrylic acid) (PAA)).[16] The trilayers approach could lead to fast film growth and had a high MMT content in the coating. Furthermore, Li et al. carried out a comprehensive evaluation of various MMT filled LbL coating formulation on the fire performance, mechanical and physical properties of FPU foam according to trilayers's approach.[18] Therefore, it is an effective method to fabricate a flame retardant coating on FPU foam using the trilayers approach.

In our present work, the titanate nanotubes filled coating was fabricated on FPU foam using the trilayers approach (chitosan/titanate nanotubes/alginate). Titanate nanotubes can show excellent protective effect owing to its high surface area, insulating barrier effect and excellent adsorption effect. The original idea of this work was to enhance this protective effect of titanate nanotubes owing to its only presence on FPU foam surface. The flame retardant and smoke suppression properties of coated FPU foams were emphatically studied by cone calorimetry. As can be expected, the titanate nanotubes filled coating can improve the flame retardant and smoke suppression properties of FPU foam and reduce its fire hazard.

EXPERIMENTAL SECTION

Materials. The commercial flexible polyurethane foam without any flame-retardant additives (polyether type, DW30) was provided by Jiangsu Lvyuan New Material Co., Ltd. Chitosan (degree of deacetylation 80−95%) and alginate were supplied by Sinopharm Chemical Reagent Co. Ltd. Titanium dioxide (anatase), sodium hydroxide (NaOH), tetramethylammonium hydroxide (TMAOH, 25% aqueous solution) and hydrochloric acid (HCl 36−38%) were also provided by Sinopharm Chemical Reagent Co. Ltd. (Shanghai, China). Polyacrylic acid (PAA, Mw ∼ 100 000) was supplied by Sigma-Aldrich. Deionized water (18.2 MΩ, pH = 6) was used for all experiments unless otherwise stated.

Preparation of Titanate Nanotubes. Titanate nanotubes were prepared by a hydrothermal method described elsewhere.[20] First, 2 g of anatase-type titanium dioxide powders was dispersed in 40 mL of 10 M NaOH solution. The resulting suspension was heated in a sealed Teflon autoclave at 150 °C for 48 h. After the reaction, the produced precipitate was treated with 0.1 M HCl solution and deionized water. Afterward, the precipitate was dispersed in 1 M HCl solution, then stirred for 15 h to further proton exchange. Then, the precipitate was separated by centrifugation and washing with distilled water until the PH value of the supernatant become natural. A white product was obtained after drying at 60 °C for 24 h.

Preparation of Solution. The titanate nanotubes suspension was prepared according to a previous report.[21] Titanate nanotubes (2 or 8 $mg{\cdot}mL^{-1}$) were dispersed in 0.2 M tetramethylammonium hydroxide (TMAOH) aqueous solution, and then the mixture was stirred for 24 h to produce a translucent colloidal titanate nanotubes suspension. Alginate (3 $mg{\cdot}mL^{-1}$) solution was prepared by introducing alginate into deionized water, and then the mixture was stirred for 24 h.

dx.doi.org/10.1021/am507045g | ACS Appl. Mater. Interfaces 2015, 7, 101−111

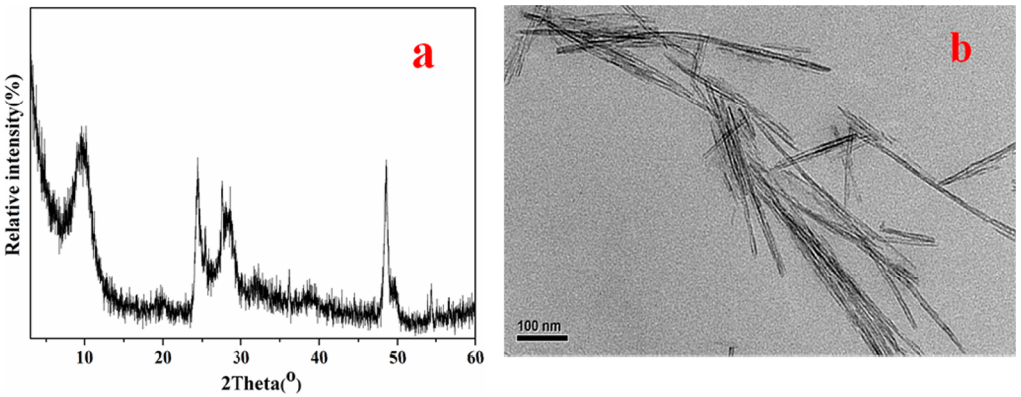

Figure 1. XRD pattern (a) and TEM image (b) of titanate nanotubes.

Chitosan solution (5 mg·mL^{-1}) was prepared by adding chitosan to deionized water and the pH was adjusted to 5 with 1 M HCl solution, and then the mixture was stirred for 24 h.

Layer-by-Layer Assembly. First, FPU foam was presoaked in a 0.1 M HNO_3 solution for 5 min to create a positively charged surface. Afterward, FPU foam was squeezed out by hand to expel excess acid solution, then washed with deionized water. Then, the FPU foam was immersed into 1.0% PAA solution for 5 min as a primer layer to improve adhesion. The treated FPU foam was alternately immersed into chitosan solution, titanate nanotubes suspension and alginate solution. Every immersion was sustained for 2 min and then rinsed with deionized water, then wrung out by hand to expel liquid among FPU foam. When the desired trilayers number was carried out, FPU foam was dried at 60 °C overnight before testing. The preparation process could be shown in Scheme 1. Prior to deposition, a quartz slide (10 × 20 mm) was cleaned by immersing into boiling piranha solution (H_2O_2−H_2SO_4 1:3 v/v) at 85 °C for 50 min. ***Caution!*** Piranha solution is aggressive and explosive. Never mix piranha waste with solvents. Check the safety precautions before using it. Subsequently, the layer-by-layer deposition process on treated quartz slides was similar to that of FPU foam and the used concentration of chitosan solution, titanate nanotubes suspension and alginate solution is 5, 8, and 3 mg·mL^{-1}, respectively.

Measurements. X-ray diffraction (XRD) measurements of titanate nanotubes was performed with a Japan Rigaku D=Max-Ra rotating anode X-ray diffractometer equipped with a Cu Kα tube and Ni filter (λ = 0.1542 nm).

Transmission electron microscopy (TEM) images of titanate nanotubes were obtained on a Jeol JEM-100SX transmission electron microscope with an acceleration voltage of 100 kV.

UV−vis absorption measurements were taken using a UV−visible spectrophotometer (Cary 100 Bio, Varian, America).

Attenuated total reflection Fourier transform infrared (ATR-FTIR) spectra with the frequency region from 4000 to 400 cm^{-1} were recorded by a Nicolet 6700 spectrometer (Thermo-Nicolet) using 32 scans.

The morphologies of control and coated FPU foams coated with a gold layer in advance were observed using scanning electron microscopy. (SEM, AMRAY1000B, Beijing R&D Center of the Chinese Academy of sciences, China).

The thermogravimetric analysis (TGA) of samples under nitrogen atmosphere was examined on a TGA-Q5000 apparatus (TA Company, USA) from 50 to 700 °C at a heating rate of 20 °C/min.

The combustion test was performed on the cone calorimeter (Fire Testing Technology, UK) tests according to ISO 5660 standard procedures, with 100 × 100 × 25 mm specimens. Each specimen was exposed horizontally to 35 kW/m^2 external heat flux.

Thermogravimetric analysis/infrared spectrometry (TG-IR) of the samples was performed using a TGA Q5000 IR thermogravimetric analyzer that was interfaced to the Nicolet 6700 FTIR spectrophotometer through a Thermo-Nicolet TGA special connector.

Laser Raman spectroscopy measurements of char residue of samples after the cone test were performed with a SPEX-1403 laser Raman spectrometer (SPEX Co., USA).

RESULTS AND DISCUSSION

Characterization of Titanate Nanotubes, Titanate Nanotubes Filled Multilayers and Coated FPU Foams. Figure 1a depicts the typical XRD pattern of titanate nanotubes after acid treatment. Peng et al. pointed out that titanate nanotubes are constructed from scrolled trititanate ($H_2Ti_3O_7$) sheets, but Ma et al. reported that the nanotubes are composed of lepidocrocite sheets.[10,11,20] Thus, there is still controversy for the exact crystal structure of the nanotubes. However, they both indicated that the crystal structure is hydrogen titanate. Our XRD pattern of titanate nanotubes is similar to their reports, so the as-synthesized nanotubes have the hydrogen titanate structure. The TEM image of titanate nanotubes is shown in Figure 1b. The titanate nanotubes have a typical crystal size with a 10 nm outer diameter, 6 nm inner diameter and several hundred nm length.

UV−vis absorption spectrometry was used to monitor the coating growth on the quartz slides substrate. The UV−vis absorption spectra of 4, 6, 8, 10 and 12 trilayers prepared on quartz slides are shown in Figure 2. It is found that the absorption in the spectral range of 240−340 nm increases with the increases of the trilayers number. Additionally, the

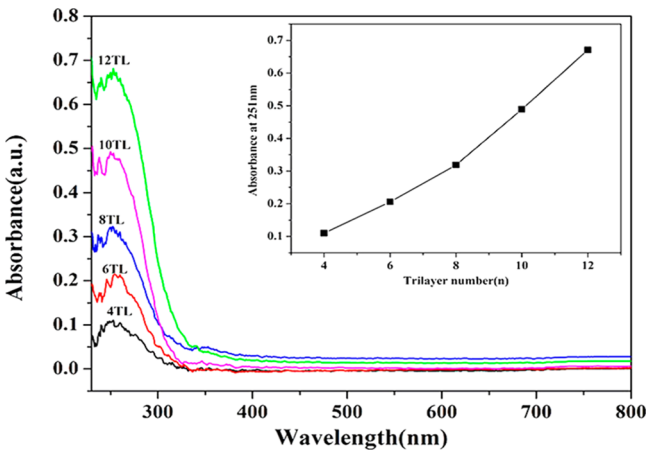

Figure 2. UV−vis absorption spectra of chitosan/titanate nanotubes/alginate multilayers on quartz slides. The inset plot shows the absorption intensity at 251 nm relative to the trilayers number.

dx.doi.org/10.1021/am507045g | ACS Appl. Mater. Interfaces 2015, 7, 101−111

Table 1. Weight Gain of Coating Mass on FPU Foams as a Function of the Concentration of Titanate Nanotubes Suspension and Trilayers Number

sample	trilayers number (n)	titanate nanotubes (mg·mL^{-1})	chitosan (mg·mL^{-1})	alginate (mg·mL^{-1})	weight gain of coating mass (% wt)
FPU0	0	0	0	0	0
FPU1	2	2	5	3	0.72
FPU2	4	2	5	3	0.95
FPU3	8	2	5	3	1.70
FPU4	2	8	5	3	1.53
FPU5	4	8	5	3	3.60
FPU6	8	8	5	3	5.65

absorption peak at 251 nm is ascribed to the absorption of titanate nanotubes.[13] As shown in the inset plot, the absorption intensity at 251 nm shows an almost linear increase relative to the deposited trilayers number, indicating that almost the same amount of titanate nanotubes was deposited on the quartz slides substrate at each assembly cycle.[21]

Table 1 gives the weight gain of coating mass on FPU foams as a function of the concentration of titanate nanotubes suspension and trilayers number. The control and coated FPU foams are marked as FPU0, FPU1, FPU2, FPU3, FPU4, FPU5 and FPU6, and the corresponding weight gain is 0%, 0.72%, 0.95%, 1.70%, 1.53%, 3.60% and 5.65%, respectively. The weight gain shows an almost linear growth trend relative to the trilayers number and, moreover, shows the dependence on the concentration of titanate nanotubes suspension.[22−24] Such a result can give an indication that the loading of titanate nanotubes prepared on FPU foam can be modified by changing the concentration of titanate nanotubes suspension and trilayers number.

ATR-FTIR spectroscopy can be used to qualitatively determine the surface chemical structures of control and coated FPU foams. Figure 3 shows the ATR-FTIR spectra of all

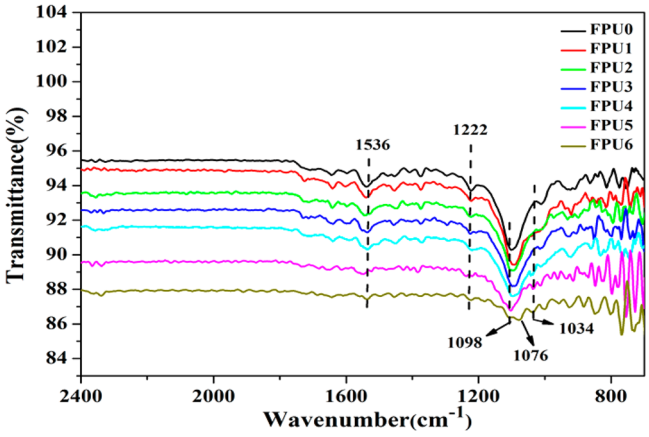

Figure 3. ATR-FTIR spectra of control and coated FPU foams.

samples. The absorption peaks at 1098, 1222 and 1536 cm^{-1} are attributed to the nonsymmetric stretching vibration of C−O−C, the stretching vibration of aromatic C−O, deformation and stretching vibrations of N−H in FPU foam, respectively.[25,26] The intensity of the absorbance at the three bands are all decreased with the increases of coating mass, which can be ascribed to the overlay of titanate nanotube filled coating. For FPU4, FPU5 and FPU6, there are two new peaks at 1077 and 1034 cm^{-1}, which is corresponding to C−O stretching for the chitosan structure unit and C−O−C stretching for the alginate structure unit, respectively.[27] Therefore, the ATR-FTIR results confirm the presence of chitosan and alginate in the deposited coating.

The surface morphologies of the FPU foams are presented in Figure 4. Selected images of the samples with 8 trilayers prepared from two different concentration of titanate nanotubes suspension are provided as representative images. The SEM image of FPU0 in Figure 4a reveals the complex and irregular architecture, which has a reported 50−70% open-celled structure. At high magnification (Figure 4b), the FPU0 sample has a smooth and clean surface. The two coated FPU foams (FPU3 and FPU6) have uniform nanotexture throughout the foam thickness without altering the macroscale porosity of the foam, indicating the conformal nature of LbL deposition. A rough surface can be observed for the two coated FPU foams owing to the presence of a titanate nanotube filled coating, as shown in Figure 4d,g. For FPU3, the outline of titanate nanotubes can be clearly observed, as shown in Figure 4e. Furthermore, titanate nanotubes are distributed well on the wall of FPU foam. It is worthy to discuss the image of FPU6 in Figure 4h. Nanometer scale titanate nanotubes are coated well along the entire wall of FPU foam and show a randomly oriented and entangled network structure. Grunlan and his co-workers have previously constructed multiwalled carbon nanotube (MWCNTs) filled coating on FPU foam using the trilayers approach (polyethylenimine (PEI)/MWCNTs/poly-(acrylic acid) (PAA)). The MWCNTs were completely embedded and were very well distributed in the PAA/PEI filled polymeric coating, and the mass fraction % MWCNTs was about 51 wt %.[17] The reason can be attributed to the exponential coating growth in the PAA/PEI based bilayers system.[28,29] However, in our present work, the images that titanate nanotubes embedded into chitosan/alginate filled coating cannot be observed. It may be attributed to low linear coating growth in the chitosan/alginate based bilayers system owing to the hindrance of rigid polysaccharides chains during adsorption process.[30] Here, a specific experiment was carried out in order to get the information about coating growth. Titanate nanotubes were alternately dispersed into chitosan solution (5 mg·mL^{-1}) and alginate solution (3 mg·mL^{-1}). Each one was sustained for 2 min and titanate nanotubes were separated by centrifugation and followed by rinsing with deionized water, then separated by centrifugation again. The process was repeated until 8 deposition cycles were carried out. The TEM image of the treated titanate nanotubes is shown in Figure S1 (Supporting Information). It can be found that outside wall of titanate nanotubes was coated with a thin polymeric coating, which should come from the deposition of the chitosan/alginate filled coating. Furthermore, some island like apophysis are also observed. Therefore, the chitosan/alginate filled coating can effectively adhere to the wall surface of titanate nanotubes. Combining this information with the

dx.doi.org/10.1021/am507045g | ACS Appl. Mater. Interfaces 2015, 7, 101−111

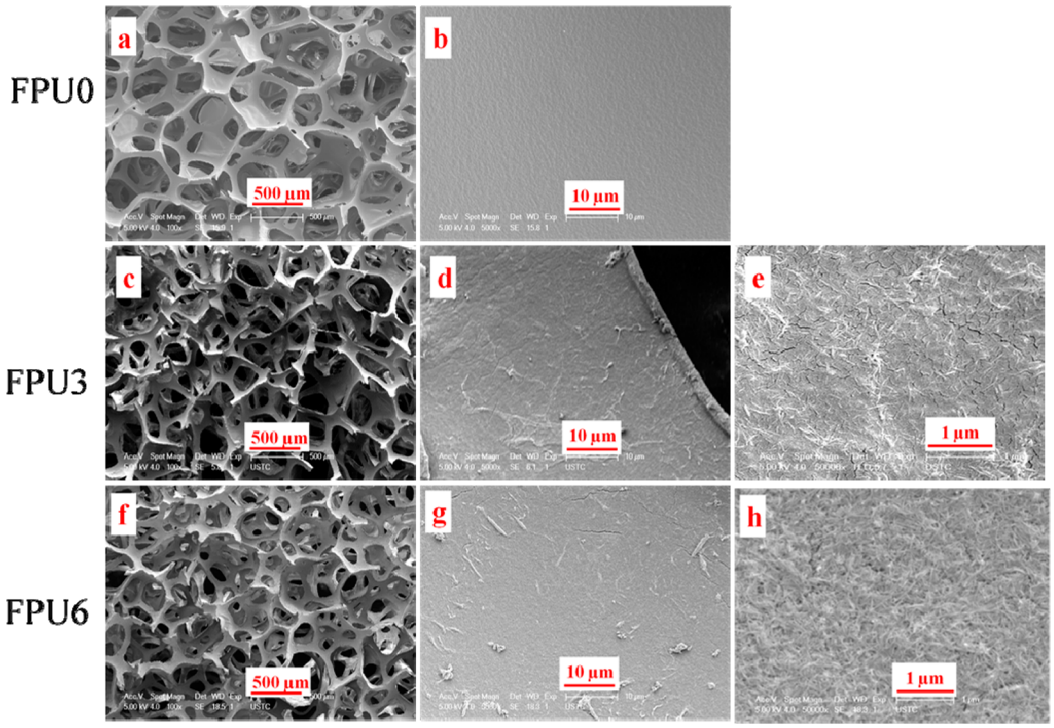

Figure 4. SEM images of FPU0 (a and b), FPU3 (c, d and e) and FPU6 (f, g and h), respectively.

initial discussion of the SEM image, we can assert that chitosan/alginate filled coating mainly acts as a binder to hold titanate nanotubes together instead of forming polymeric coating on FPU foam surface. Therefore, high content of titanate nanotubes in the coating can be obtained, which would be further confirmed by the following TGA result.

Thermal Stability. Figure 5 presents the experimental TGA curves of all samples under nitrogen atmosphere. As can be

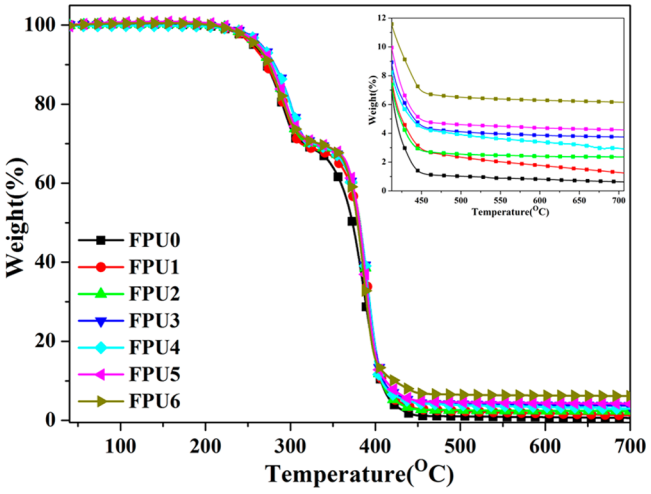

Figure 5. TGA curves of control and coated FPU foams under nitrogen atmosphere.

observed, FPU0 has two thermal degradation steps. The first stage shows about a 29% mass loss in the temperature range from 190 to 308 °C. It is attributed to the liberation of the diisocyanate compound, which is caused by depolymerization of the urethane and the bisubstituted urea groups. Another step is ascribed to the pyrolysis of the remaining polyether chain.[31] FPU0 occurs with almost no char residue left. Coated FPU foams also have two thermal decomposition steps but have obvious high char residue, which can indicate the titanate nanotubes content with respect to the FPU foam.[18] The char residue at 700 °C is 0.62%, 1.28%, 2.35%, 3.75%, 2.94%, 4.24% and 6.16% for FPU0, FPU1, FPU2, FPU3, FPU4, FPU5 and FPU6 samples, respectively, indicating the high titanate nanotubes content in the coating that prepared on FPU foam.

Flammability. *Cone Calorimeter Test.* Owing to its applications in real fire disasters, cone calorimetry is widely used to reveal the combustion behavior of a material in a real fire scenario. Many combustion parameters such as peak heat release rate, total heat release, smoke production rate, total smoke release and carbon monoxide production are employed to evaluate the potential fire hazard of a material.

Heat Release Rate (HRR) and Total Heat Release (THR). The HRR, especially for the peak HRR value, is usually considered to be key parameter to measure fire safety. In general, the peak HRR represents the point in a fire where heat is likely to propagate further or ignite adjacent objects, so its reduction is important for fire safety. The HRR and THR curves are presented in Figure 6a,b, and the corresponding data are shown in Table 2. It is found that the HRR curves of FPU0 show two steps of heat release. The first step represents the pyrolysis of diisocyanate compound, and the second step represents the pyrolysis of polyol.[32,33] As show in Table 2, all coated FPU foams show the peak HRR reduction compared with that of FPU0, indicating the enhancement of flame retardancy for coated FPU foams. Especially for the FPU6 sample with only a 5.65% mass gain, its peak HRR is 209 kW/m^2, with a high reduction of 70.2% compared with that of FPU0 (714 kW/m^2). Moreover, the FPU6 sample almost eliminates the second peak and largely extends the time it takes for complete combustion to occur. The great improved flame retardancy should be attributed to the protective effect of

dx.doi.org/10.1021/am507045g | ACS Appl. Mater. Interfaces 2015, 7, 101−111

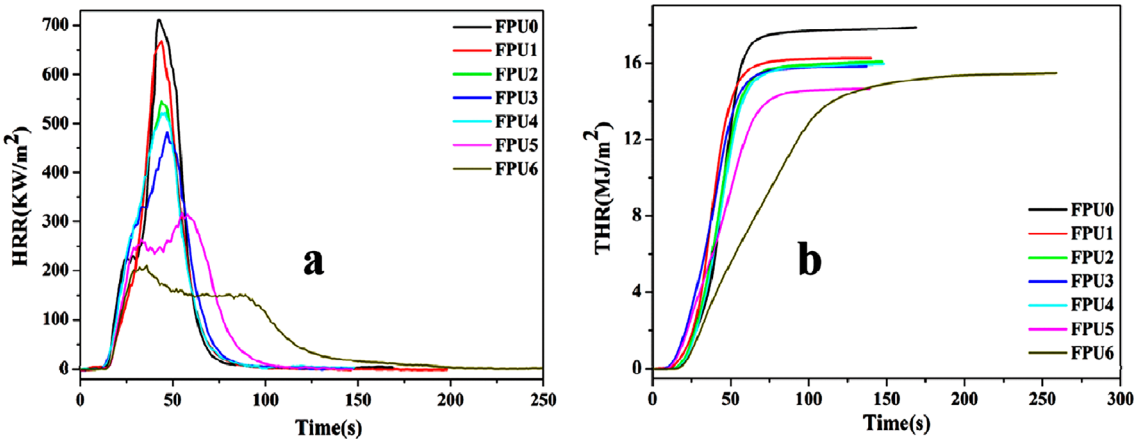

Figure 6. Heat release rate (a) and total heat release (b) curves of control and coated FPU foams.

Table 2. Cone Data of Control and Coated FPU Foams

sample	time to ignition (s)	peak HRR (kW/m^2)	THR (MJ/m^2)	peak SPR (m^2/s)	TSR (m^2/m^2)	peak CO production (g/s)	FPI ((m^2·s)/kW)
FPU0	2	714	17.8	0.0875	203.3	0.0143	0.00281
FPU1	2	667	16.3	0.0778	205.4	0.0139	0.00299
FPU2	2	545	16.1	0.0885	201.3	0.0147	0.00367
FPU3	2	482	15.8	0.0894	194.2	0.0126	0.00415
FPU4	2	521	16.0	0.0851	197.3	0.0122	0.00384
FPU5	3	316	14.9	0.0611	191.8	0.00888	0.00949
FPU6	3	212	15.5	0.0325	120.1	0.00521	0.0142

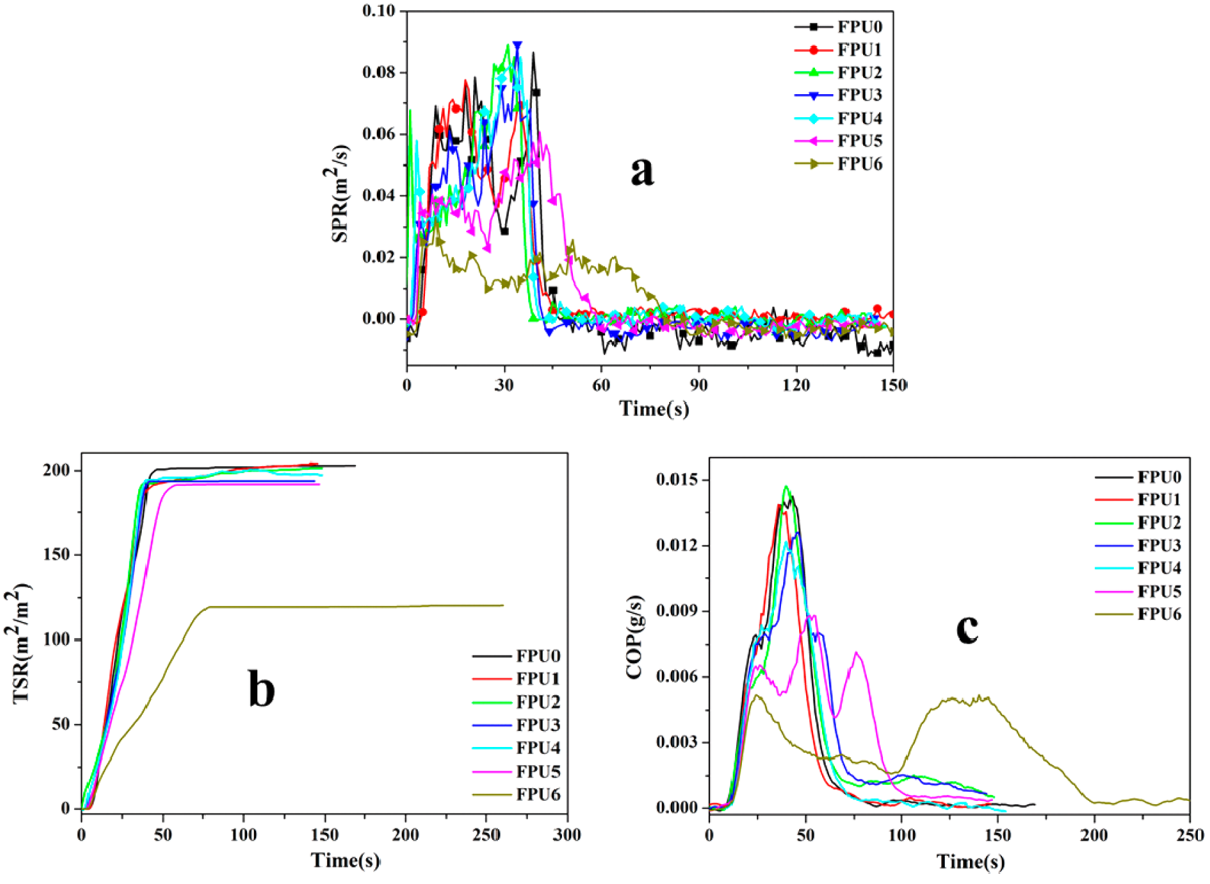

Figure 7. Smoke production rate (a), total smoke release (b) and carbon monoxide production (c) curves of control and coated FPU foams.

titanate nanotubes network structure formed, which can effectively slow down the heat and mass transfer between gas and condensed phases, and prevent the underlying material from further combustion. Here, it is necessary to give a

dx.doi.org/10.1021/am507045g | ACS Appl. Mater. Interfaces 2015, 7, 101−111

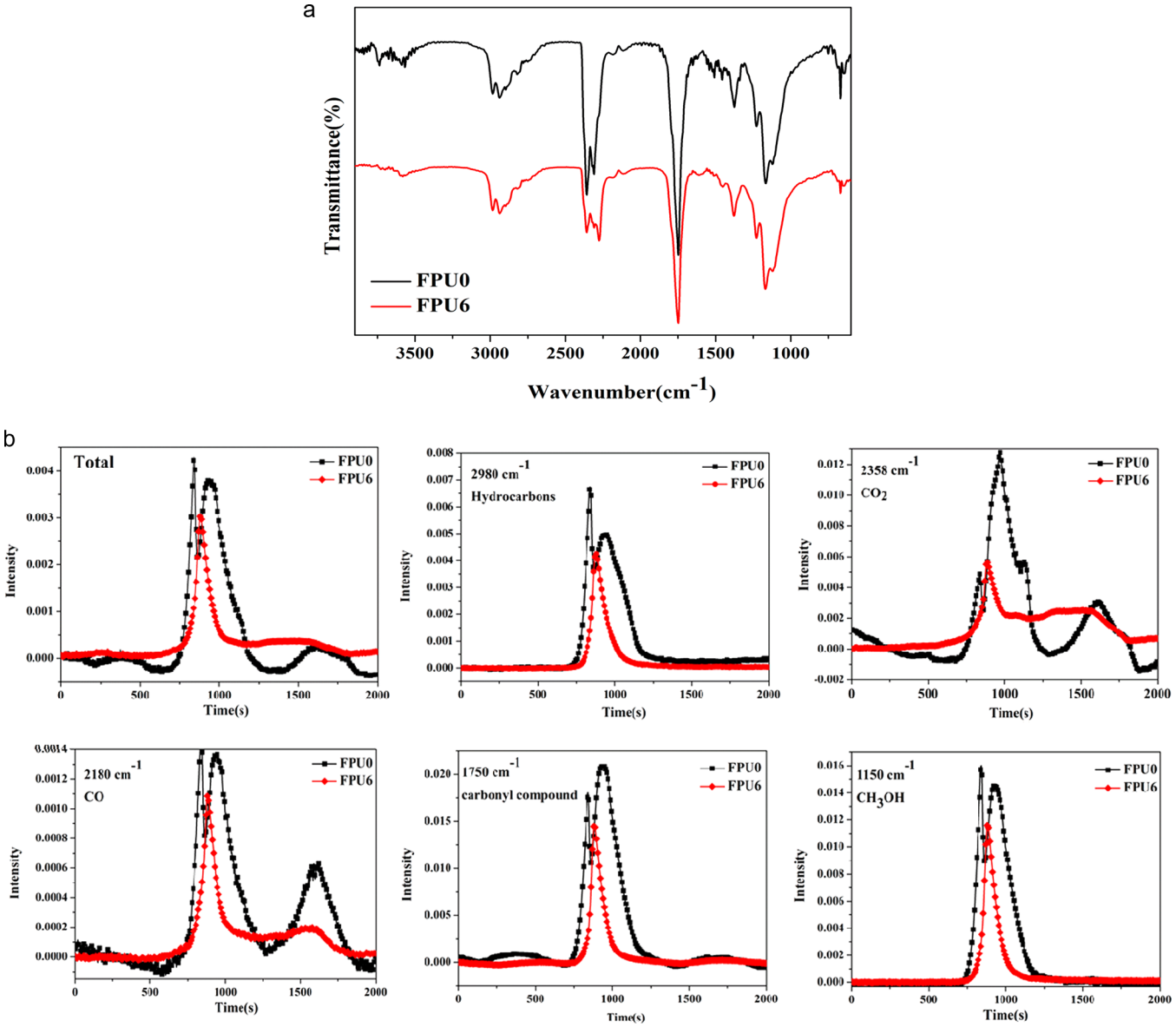

Figure 8. (a) FTIR spectra of volatilized pyrolysis products emitted from FPU0 and FPU6 at maximum evolution rate. (b) Intensity of characteristic peaks of volatilized pyrolysis products of FPU0 and FPU6.

comparison between our present work and Grunlan's group previous work.[17,18] Grunlan's group mainly focused on fabricating MMT and MWCNTs filled coating on FPU foam using trilayers approach (polyethylenimine (PEI)/MMT or MWCNTs/poly(acrylic acid) (PAA)). They found that 10% (minimum threshold) or more MMT filled coating mass gain only can significantly reduce the FPU foam flammability (eliminate the second peak HRR) and the FPU foam with (3.4 ± 0.4) % MWCNTs filled coating mass gain showed only 35 ± 3% reduction in peak HRR. Furthermore, the coating composed of high PEI/PAA content (~50%), which is the highly combustible component, results in the deterioration of the mechanical properties of FPU foams. In our present work, the coating with high content of flame retardant composition (titanate nanotubes) can be deposited on the surface of FPU foam. Only 5.65% coating mass gain can have great improvement in flame retardancy for FPU foam.

Another obvious result is that the improved flame retardancy shows dependence on the trilayers number and the concentration of titanate nanotubes suspension, as shown in Table 2. The higher trilayers number and the concentration of titanate nanotubes suspension, the greater reduction in peak HRR. Additionally, THR of coated FPU foams have some slight reduction, indicating that the titanate nanotubes formed network structure mainly acts as a protective layer to slow down the heat release but not significantly decrease the final total heat release.

Smoke Production Rate (SPR), Total Smoke Release (TSR) and Carbon Monoxide (CO) Production. It should be noted that the real killer in fires is the smoke and volatiles produced rather than the heat of the fire itself. The smoke, smoke particulates and some toxic compounds (especially CO) are known to cause a large number of the fatalities during the scenario of a real fire. Therefore, it will be significant for reducing the amount of smoke and carbon monoxide formed during burning. The SPR, TSR and CO production curves are presented in Figure 7, and the related data are shown in Table 2. As shown in Figure 7a, only FPU5 and FPU6 samples have

dx.doi.org/10.1021/am507045g | ACS Appl. Mater. Interfaces 2015, 7, 101−111

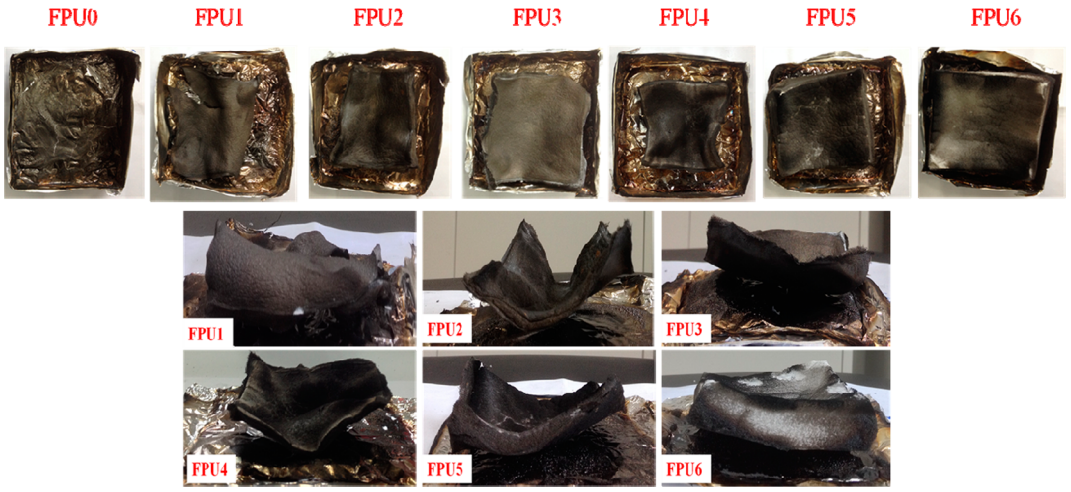

Figure 9. Digital photos of char residue of control and coated FPU foams after the cone test.

obvious reduction in SPR values in all the combustion process compared to FPU0, which can be ascribed to enough titanate nanotubes content that prepared on FPU foam. The peak SPR value of FPU5 and FPU6 is 0.0611 and 0.0325 m^2/s, respectively, with the reduction of 30.2% and 62.8% as compared to that (0.0875 m^2/s) of FPU0, indicating that the nanotubes formed network structure can act as an effective protective layer to slow down the release of combustible gases and smoke-forming materials. It is worthy to note that the reduction in SPR for FPU6 is accompanied by a pronounced prolongation of burning time with a flat curve, which is attributed to the highly effective protective effect of the network structure formed (a sufficient amount of titanate nanotubes covered the entire surface of FPU foam, as seen from the SEM image). The TSR curves of all FPU foams are shown in Figure7b. Here, the meaning of TSR is cumulative smoke produced per unit area of the sample. The TSR values of all coated FPU foams except FPU1 decrease with respect to FPU0. Especially for the FPU6 sample, its TSR value is only 120 m^2/m^2, which is 40.9% less than that (203 m^2/m^2) of FPU0, indicating the excellent smoke suppression effect. Figure7c shows the CO production curves for all samples in the cone test. Similar to the trend of HRR, the reduction in peak value and delayed release for CO production can be observed, indicating the great efficiency in inhibiting the release of toxic compounds during burning. As a result, the reduction of smoke and toxic gas is contributed to improve the fire safety of FPU foam.

Fire Performance Index (FPI). FPI is defined as the ratio of time to ignition and peak HRR value. It is often used to give an overall evaluation of the fire safety of a material in the cone test. Generally speaking, the greater the value of FPI, the higher fire safety has the material. Table 2 shows the FPI values of all samples. It can be found that the FPI values also show the dependence on the number of trilayers and concentration of titanate nanotubes suspension. FPU6 has highest FPI value, 0.0142, so it has the highest fire rescue.

Flame Retardant Mechanism. To understand the mechanism of the improved fire safe by the nanotubes filled coating, the volatilized products were investigated using the thermogravimetric analysis/infrared spectrometry (TGA-IR). Figure 8a presents the FTIR spectra of volatilized pyrolysis products of control FPU0 and FPU6 at the maximum decomposition rates. It is found that the absorption peaks of the pyrolysis products of the FPU6 sample are identical to that of FPU0, indicating that the deposited coating does not alter the thermal decomposition process significantly. Some of the volatilized pyrolysis products of FPU foam can be identified by FTIR signals: the bands at 3400−3790 cm^{-1} are assigned to the stretching vibration of O—H, indicating the release of water. The bands at 2930−2982 cm^{-1} are ascribed to the aliphatic C—H bonding coming from various alkanes; the peak at 2358 cm^{-1} is assigned to the stretching vibration of carbon dioxide; the characteristic peak at 1753 cm^{-1} is due to the absorbance of stretching vibration of C═O group; the peaks at 1378 and 1170 cm^{-1} are caused by the C—O bond arising from ethers.

To further understand the mechanism of improved fire safety for coated FPU foams, the absorbance of pyrolysis products of FPU0 and FPU6 as a function of temperature is revealed in Figure 8b. The selected volatilized pyrolysis products are studied, including CH_3OH (1167 cm^{-1}), carbonyl compounds (1751m^{-1}), CO (2180 cm^{-1}) and CO_2 (2358 cm^{-1}). The absorption intensity of volatilized products of FPU6 sample is less than that of FPU0, especially for CO_2, just as shown in Figure 8b. The reduced amount of the organic volatiles means less "fuel" to be fed back to the flame, which can be indicated from the reduction in HRR and THR values during the cone test. Additionally, the reduced amount of these organic volatiles further results in the inhibition of smoke due to that the organic volatiles may crack into smaller hydrocarbon molecules and smoke particles, which can be further condensed or aggregated to form smoke.[7,34] Therefore, the decrease of peak SPR and TSR can be observed in the cone test.

The physical barrier effect and adsorption effect of titanate nanotubes are considered to be the possible reasons for the reduction of organic volatiles. Titanate nanotubes can form a randomly oriented and entangled network structure, which can act as a physical barrier to delay the evolution of organic volatiles. Additionally, titanate nanotubes have a large specific surface area and tubular structure, thus some radicals and small gaseous molecules can be trapped on the surface or inside of the nanotubes. This can provide an environment in which radicals have more of an opportunity to undergo radical transfer and recombination reactions, further condensed or aggregated into solid char on the surrounding nanotubes, thereby reducing the amount of organic volatiles.

In general, the effective char residue with the characteristics of faster forming, denser, thicker and/or less cracks can indicate

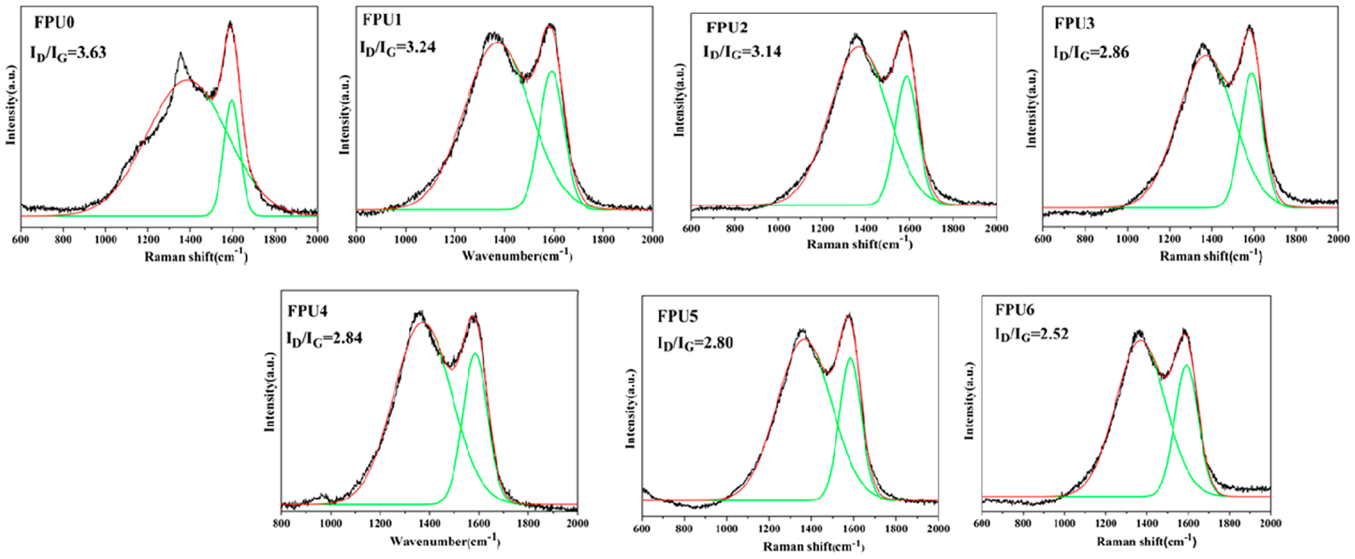

Figure 10. Raman spectra of char residue of control and coated FPU foams after cone test.

the great improved fire safety for a polymeric material.[35] The digital photos of the char residue of all samples after the cone test are shown in Figure 9. As can be observed, control FPU foam is a highly flammable material, almost leaving no char residue after combustion. All coated FPU foams show relatively high char residue, but show some differences. Compared to thin residual char for FPU1, the FPU2, FPU3 and FPU4 samples show thicker char residue, but all have some curl. The smaller curl can be observed for the residual char of FPU5. As for the FPU6 sample, its residual char is thickest and has little to no imperfections, basically retaining the original shape of the unburned FPU foam, which is why it is so effective at decreasing and maintaining low combustion parameters throughout the cone test.

Raman spectroscopy is a useful measurement to characterize graphitic structure of char residue of a polymeric material. The Raman spectra of char residue of all samples after cone calorimeter test are shown in Figure 10. All samples show two visible bands. The band at 1580 cm^{-1} is the G-band, which is corresponded to an E_{2g} mode of hexagonal graphite and is related to the vibration of sp^2-bonds carbon atoms in graphite layers. The other band at 1350 cm^{-1} is D-band, which is associated with vibration of carbon atoms with dangling bonds in the plane terminations of disordered graphite or glass carbons.[36] The graphitization degree of char residue is estimated by the ratio of the intensity of the D and G bands (I_D/I_G), where I_D and I_G are the integrated intensities of the D and G bands, respectively. Basically, the lower the ratio of I_D/I_G, the better the structure of the char. According to Figure 10, the I_D/I_G ratio follows the order: FPU0 > FPU1 > FPU2 > FPU3 > FPU4 > FPU5 > FPU6. Therefore, the char residues of all coated FPU foams have a higher graphitization degree than that of FPU0. The char residue with high graphitization degree can act as an effective barrier to retard the evolution of flammable volatilized products, the oxygen and heat ingress to the condensed phase and mass transfer into combustion zone.

In summary, the possible mechanism of the improved fire safety for coated FPU foams is proposed as follows: by combining with physically insulating barrier effect and adsorption effect of titanate nanotubes, the formed network structure shows an excellent protective effect to slow down the foam pyrolysis and reduce evolution of mass into the gas phase, thus reduce the amount of organic volatiles. At the same time, the further formed char residue with high graphitization degree provides an effective protective shield that results in a reduction in heat, oxygen and mass transfers between the flame and underlying material.

CONCLUSION

The layer-by-layer assembled coating consisting of chitosan, titanate nanotubes and alginate was successfully deposited on a flexible polyurethane foam surface to improve its flame retardant and smoke suppression properties. By altering the concentration of titanate nanotubes suspension and trilayers number, the content of titanate nanotubes prepared on FPU foam was changed. Characterization by means of ATR-FTIR spectra and SEM images showed a homogeneous dispersion and random entanglement of titanate nanotubes filled coating prepared on the surface of FPU foam. Incorporation of titanate nanotubes filled coating can remarkably enhance fire safety properties of FPU foams, including the improved flame retardant and smoke suppression properties. The coated foam with only 5.65% mass gain showed great reduction in peak heat release rate (70.2%), peak smoke production rate (62.8%), total smoke release (40.9%) and peak carbon monoxide production (63.5%). The physically insulating barrier and adsorption effect of titanate nanotubes were considered the reasons for the improvement in flame retardant and smoke suppression properties. The effects can slow down the foam pyrolysis and reduce the amount of organic volatiles, further resulting in a reduction in heat, oxygen and mass transfers between the flame and underlying material.

ASSOCIATED CONTENT

Supporting Information

Figure S1: TEM images of tianate nanotubes after treated with chitosan/alginate bilayer. This material is available free of charge via the Internet at http://pubs.acs.org.

dx.doi.org/10.1021/am507045g | ACS Appl. Mater. Interfaces 2015, 7, 101−111

AUTHOR INFORMATION

Corresponding Authors

*Yuan Hu. Fax/Tel: +86-551-63601664. E-mail: yuanhu@ustc.edu.cn.

*Lei Song. Fax/Tel: +86-551-63601664. E-mail: leisong@ustc.edu.cn.

Notes

The authors declare no competing financial interest.

ACKNOWLEDGMENTS

The work was financially supported by National Basic Research Program of China (973 Program) (2012CB719701), National Key Technology R&D Program (2013BAJ01B05), National Natural Science Foundation of China (51303167), National Natural Science Foundation of China (51276054) and National Natural Science Foundation of China (51303165).

REFERENCES

(1) Serpone, N.; Lawless, D.; Khairutdinov, R. Size Effects on the Photophysical Properties of Colloidal Anatase TiO_2 Particles: Size Quantization versus Direct Transitions in this Indirect Semiconductor? *J. Phys. Chem.* **1995**, *99*, 16646−16654.

(2) Beecroft, L. L.; Ober, C. K. Novel Ceramic Particle Synthesis for Optical Applications: Dispersion Polymerized Preceramic Polymers as Size Templates for Fine Ceramic Powders. *Adv. Mater.* **1995**, *7*, 1009−1012.

(3) Bavykin, D. V.; Milsom, E. V.; Marken, F.; Kim, D. H.; Marsha, D. H.; Riley, F. C.; Walsh, D. J.; El-Abiary, K. H.; Lapkin, A. A. The Oxidation of Borohydride Ion at Titanate Nanotube Supported Gold Electrodes. *Electrochem. Commun.* **2006**, *8*, 1655−1660.

(4) Ntho, T. A.; Anderson, J. A.; Scurrell, M. S. CO Oxidation over Titanate Nanotube Supported Au: Deactivation due to Bicarbonate. *J. Catal.* **2009**, *261*, 94−100.

(5) Tang, Z. R.; Yin, X.; Zhang, Y.; Xu, Y. J. Synthesis of Titanate Nanotube-CdS Nanocomposites with Enhanced Visible Light Photocatalytic Activity. *Inorg. Chem.* **2013**, *52*, 11758−11766.

(6) Wu, Y.; Song, L.; Hu, Y. Fabrication and Characterization of TiO_2 Nanotube-Epoxy Nanocomposites. *Ind. Eng. Chem. Res.* **2011**, *50*, 11988−11995.

(7) Dong, Y. Y.; Gui, Z.; Hu, Y. The Influence of Titanate Nanotube on the Improved Thermal Properties and the Smoke Suppression in Poly(methyl methacrylate). *J. Hazard. Mater.* **2012**, *209*, 34−39.

(8) Sharma, R. K.; Bhatnagar, M. C.; Sharma, G. L. Mechanism in Nb Doped Titania Oxygen Gas Sensor. *Sens. Actuators, B* **1998**, *46*, 194−201.

(9) Sotter, E.; Vilanova, X. Development of a Thick Film Gas Sensor for Oxygen Detection at Trace Levels. Ph.D. Thesis, University of Rovira and Virgili, Tarragona, Spain, 2006.

(10) Chen, Q.; Du, G. H.; Zhang, S.; Peng, L. M. The Structure of Trititanate Nanotubes. *Acta Crystallogr., Sect. B: Struct. Sci.* **2002**, *58*, 587−593.

(11) Chen, Q.; Du, G. H.; Che, R. C.; Yan, Z. Y.; Peng, M. Preparation and Structure Analysis of Titanium Oxide Nanotubes. *Appl. Phys. Lett.* **2001**, *79*, 3702−3704.

(12) Zhang, C.; Jiang, X.; Tian, B.; Wang, X.; Zhang, X.; Du, Z. Modification and Assembly of Titanate Sodium Nanotubes. *Colloids Surf., A* **2005**, *257*, 521−524.

(13) Ma, R.; Sasaki, T.; Bando, Y. Layer-by-Layer Assembled Multilayer Film of Titanate Nanotubes, Ag- or Au-Loaded Nanotubes and Nanotubes/Nanosheets with Polycations. *J. Am. Chem. Soc.* **2004**, *126*, 10382−10388.

(14) Grandcolas, M.; Louvet, A.; Keller, N.; Keller, V. Layer-by-Layer Deposited Titanate-based Nanotubes for Solar Photocatalytic Removal of Chemical Warfare Agents from Textiles. *Angew. Chem.* **2009**, *121*, 167−170.

(15) Kim, Y. S.; Davis, R.; Cain, A. A.; Grunlan, J. C. Development of Layer-by-Layer Assembled Carbon Nanofiber-Filled Coatings to Reduce Polyurethane Foam Flammability. *Polymer* **2011**, *52*, 2847−2855.

(16) Kim, Y. S.; Harris, R.; Davis, R. Innovative Approach to Rapid Growth of Highly Clay-Filled Coatings on Porous Polyurethane Foam. *ACS Macro Lett.* **2012**, *1*, 820−824.

(17) Kim, Y. S.; Davis, R. Multi-Walled Carbon Nanotube Layer-by-Layer Coatings with a Trilayers Structure to Reduce Foam Fammability. *Thin Solid Films* **2014**, *550*, 184−189.

(18) Li, Y. C.; Kim, Y. S.; Shields, J.; Davis, R. Controlling Polyurethane Foam Flammability and Mechanical Behaviour by Tailoring the Composition of Clay-based Multilayer Nanocoatings. *J. Mater. Chem. A* **2013**, *1*, 12987−12997.

(19) Cain, A. A.; Nolen, C. R.; Li, Y. C. Phosphorous-Filled Nanobrick Wall Multilayer Thin Film Eliminates Polyurethane Melt Dripping and Reduces Heat Release Associated with Fire. *Polym. Degrad. Stab.* **2013**, *98*, 2645−2652.

(20) Ma, R.; Bando, Y.; Sasaki, T. Directly Rolling Nanosheets into Nanotubes. *Chem. Phys. Lett.* **2003**, *380*, 577−582.

(21) Tokudome, H.; Miyauchi, M. Titanate Nanotube Thin Films via Alternate Layer Deposition. *Chem. Commun.* **2004**, *8*, 958−959.

(22) Zhang, T.; Yan, H. Q.; Peng, M.; Wang, L. L.; Ding, H. L.; Fang, Z. P. Construction of Flame Retardant Nanocoating on Ramie Fabric via Layer-by-Layer Assembly of Carbon Nanotube and Ammonium Polyphosphate. *Nanoscale* **2013**, *5*, 3013−3021.

(23) Zhang, T.; Yan, H. Q.; Wang, L. L.; Ding, H. L.; Fang, Z. P. Controlled Formation of Self-Extinguishing Intumescent Coating on Ramie Fabric via Layer-by-Layer Assembly. *Ind. Eng. Chem. Res.* **2013**, *52*, 6138−614.

(24) Li, Y. C.; Schulz, J.; Mannen, S.; Delhom, C.; Condon, B.; Chang, S.; Zammarano, M.; Grunlan, J. C. Flame Retardant Behavior of Polyelectrolyte-Clay Thin Film Assemblies on Cotton Fabric. *ACS Nano* **2010**, *4*, 3325−3337.

(25) Wang, X.; Hu, Y.; Song, L.; Yang, H.; Xing, W.; Lu, H. In Situ Polymerization of Graphene Nanosheets and Polyurethane with Enhanced Mechanical and Thermal Properties. *J. Mater.Chem.* **2011**, *21*, 4222−4227.

(26) Liu, Y.; Ma, J.; Wu, T.; Wang, X.; Huang, G.; Liu, Y.; Li, H. Q. Y.; Wang, W.; Gao, J. Cost-Effective Reduced Graphene Oxide-Coated Polyurethane Sponge as a Highly Efficient and Reusable Oil-Absorbent. *ACS Appl. Mater. Interfaces* **2013**, *5*, 10018−10026.

(27) Wang, Z.; Zhang, X.; Gu, J.; Yang, H.; Nie, J.; Ma, G. Electrodeposition of Alginate/Chitosan Layer-by-Layer Composite Coatings on Titanium Substrates. *Carbohydr. Polym.* **2014**, *103*, 38−45.

(28) Yang, Y. H.; Haile, M.; Park, Y. T.; Malek, F. A.; Grunlan, J. C. Super Gas Barrier of All-Polymer Multilayer Thin Film. *Macromolecules* **2011**, *44*, 1450−1459.

(29) Podsiadlo, P.; Michel, M.; Lee, J.; Verploegen, E.; Kam, N. W. S.; Ball, V.; Lee, J.; Qi, Y.; Hart, A. J.; Hammond, P. T.; Kotov, N. A. Exponential Growth of LBL Film with Incorporated Inorganic Sheets. *Nano Lett.* **2008**, *8*, 1762−1770.

(30) Skovstrup, S.; Hansen, S. Gr.; Skrydstrup, T.; Schiøtt, B. Conformational Flexibility of Chitosan: A Molecular Modeling Study. *Biomacromolecules* **2010**, *11*, 3196−3207.

(31) Zammarano, M.; Krämer, R. H.; Harris, R.; Ohlemiller, T. J.; Shields, J. R.; Rahatekar, S. S.; Lacerda, S.; Gilman, J. W. Flammability Reduction of Flexible Polyurethane Foams via Carbon Nanofiber Network Formation. *Polym. Adv. Technol.* **2008**, *19*, 588−595.

(32) Krämer, R. H.; Zammarano, M.; Linteris, G. T.; Gedde, U. W.; Gilman, W. J. Heat Release and Structural Collapse of Flexible Polyurethane Foam. *Polym. Degrad. Stab.* **2010**, *95*, 1115−1122.

(33) Lefebvre, J.; Bastin, B.; Bras, M. L.; Duquesne, S.; Ritter, C.; Paleja, R.; Poutch, F. Flame Spread of Flexible Polyurethane Foam: Comprehensive Study. *Polym. Test.* **2004**, *23*, 281−290.

(34) Wang, L.; Song, L.; Hu, Y.; Yuen, R. K. Influence of Different Metal Oxides on the Thermal, Combustion Properties and Smoke Suppression in Ethylene−Vinyl Acetate. *Ind. Eng. Chem. Res.* **2013**, *52*, 8062−8069.

(35) Chen, L.; Wang, Y. Z. A Review on Flame Retardant Technology in China. Part I: Development of Flame Retardants. *Polym. Adv. Technol.* **2010**, *21*, 1−26.
(36) Bras, M. L.; Bourbigot, S.; Tallecand, Y. L.; Laureyns, J. Synergy in Intumescence-Application to Beta-Cyclodextrin Carbonisation Agent Intumescent Additives for Fire Retardant Polyethylene Formulations. *Polym. Degrad. Stab.* **1997**, *56*, 11−21.